Operational Evaluation of Air Quality Models

Paul D. Sampson Peter Guttorp

NRCSE

Technical Report Series

NRCSE-TRS No. 018

OPERATIONAL EVALUATION OF AIR QUALITY MODELS

Paul D. Sampson and Peter Guttorp

National Research Center for Statistics and the Environment

University of Washington, Box 351720

Seattle, WA 98195-1720

USA

Abstract

This paper addresses the modeling and analysis of tropospheric ozone monitoring data for the assessment or "operational evaluation" of grid-based photochemical air quality model predictions. We first discuss general issues in the evaluation of gridded model predictions of pollutant concentrations against point field measurements and review currently recommended procedures for model evaluation. We then propose three new diagnostic procedures for model evaluation. These are: (1) spatio-temporal model based estimation of grid cell averages for comparison with model predictions, (2) graphical depiction and comparison of spatio-temporal correlation structures determined from the field monitoring data and from model output, and (3) diagnostic decompositions of the spatial fields of differences between model predictions and monitoring based estimates of grid cell average concentrations. These concepts are illustrated using field data from the SARMAP field study for the San Joaquin Valley in California and predictions from the SARMAP Air Quality Model.

Keywords: NAAQS, Photochemical model, Spatial support, Spatial correlation, Spatial deformation, Image warping

1. Introduction

In the United States, the Code of Federal Regulations (CFR 40, Part 51) requires the use of grid-based photochemical models to evaluate the relative benefits of alternative emissions control strategies in regions judged to have "serious" or "severe" tropospheric ozone levels according to current National Ambient Air Quality Standards (NAAQS) (CFR 40, Part 50). These models—or modeling systems, comprised of emissions, atmospheric chemistry, and meteorological simulation subsystems—embody a large number of uncertainties as noted in a recent "white paper" by Lefohn et al (1998) available from the internet site of the North American Research Strategy for Tropospheric Ozone (NARSTO: http://odysseus.owt.com/Narsto/).

Model uncertainties are addressed to varying extents in different procedures for the evaluation of complex geophysical models. We have been interested in regional photochemical models such as the Urban Airshed Model (EPA 1994) and the SARMAP Air Quality Model for the San Joaquin Valley (Solomon et al 1994), and larger scale Eulerian acid deposition models such as RADM (Dennis et al 1990). Evaluation tasks include sensitivity studies, diagnostic testing, mechanistic testing, and "operational evaluation" (Dennis et al 1990, NRC 1991). Meng et al (1998) suggest that uncertainty analysis should include: (1) a sensitivity analysis of model output to variation in inputs and parameters, (2) an uncertainty analysis of the observations against which model predictions are to be compared, and (3) a statistical evaluation of the degree of overlap between the uncertainty band generated by the sensitivity analysis and that inherent in the observations themselves. It is often computationally infeasible to simulate these complex models repeatedly for sensitivity studies to variation in the very large numbers of model inputs and parameterizations, so there is a considerable emphasis on operational evaluation: the process of comparing model predictions against environmental monitoring data. There are, however, promising developments in the "automatic differentiation" of large scale models for sensitivity analysis (Hwang et al 1997).

Dennis et al. (1993) describe the aims of model evaluation as follows.

> The point of model evaluation is to establish the credibility of a model for use in decision-making. Most model applications require that the model extrapolate well beyond current precursor and primary emission conditions that could exist in any model evaluation data set. This is particularly true for issues that span the urban to global scales, such as oxidants, acidic deposition and visibility. Thus, a model evaluation needs to test the science in the models. Testing the science means looking for the "right" kind of answer (right answer for right reason and wrong answer for right reason), rather than simply looking for good comparisons of final outcome.

The authors note that several different tests are needed to develop judgements regarding model skill because of the spatial and temporal scales of the measurements. In their assessment of RADM they considered seasonal contrasts, spatial contrasts, and synoptic contrasts.

Literature on model evaluation notes two particular problems which have not been addressed systematically: the difficulty of comparing spatial point observations from monitoring networks with spatial averages from grid-based air quality models, and the need to assess better the ability of a model to simulate the spatial and temporal patterns of pollutant concentrations (see Seinfeld 1988, Schere 1988, Dennis et al 1990). In this paper we discuss three components of an approach to model evaluation which addresses these problems. We propose using spatio-temporal models for monitoring data to provide estimates of average concentrations over grid cells corresponding to model predictions. We next suggest the consideration and comparison of the spatio-temporal correlation structures of the environmental monitoring data and the model predictions. Finally, we propose some new diagnostic visualizations of observation–model differences.

2. Current model evaluation procedures

U.S. Environmental Protection Agency recommendations for assessing model uncertainty and accuracy are addressed broadly in Appendix W to Title 40, Part 51 of the U.S. Code of Federal Regulations (http://www.access.gpo.gov/nara/cfr). Detailed recommendations are provided in a Guidance document on Urban Airshed Model requirements for attainment demonstration (EPA 1994) and in a section of a data analysis workbook for the Photochemical Assessment Monitoring Stations (PAMS) program (http://www.epa.gov/oar/oaqps/pams/analysis/toc.html). Recommended are the following graphical displays.

• time series plots comparing hourly predicted and observed concentrations for each monitoring station,

•isopleths of observed and predicted (lowest layer) concentrations for selected hours and for daily maxima,

•scatterplots of predictions and observations,

•quantile plots,

•additional graphical displays, such as paired predictions of daily maxima.

The EPA requires the computation of three statistical summaries; these and their acceptability limits are:

•normalized accuracy of domainwide maximum 1-hr concentration *unpaired in space and time* (± 15-20 percent),

•normalized bias of all predicted and observed concentration pairs when the observation exceeds 60 ppb (± 5-15 percent),

•normalized gross error of all predicted and observed concentration pairs when the observation exceeds 60 ppb (30-35 percent).

These displays and statistics are not particularly effective at diagnosing the spatio-temporal patterns of differences between the model predictions and observational data. Furthermore, they are dependent on how one determines pairs of values to be compared, one computed from the point monitoring observational database and the other from the grid cell based model predictions.

The recommended EPA procedure (EPA 1994) for comparing observations with gridded model predictions is to use a four-cell weighted average to determine the predicted concentration to be used in comparison with observed values. We would argue that because of the spatial smoothing inherent in grid cell predictions, it is fundamentally impossible to use the model output to determine values that are (stochastically) comparable to point observations. McNair et al (1996) studied the effects of small-scale spatial variability and inhomogeneities on typical air quality model evaluation statistical measures. In view of the effects of small-scale spatial variability, we suggest here a strategy that is operationally inverse to the above EPA recommendation. Given realistic spatio-temporal statistical models of the dynamic variation for the quantities of interest, we can estimate areal (grid cell) averages from point source data for comparison with air quality model predictions—"block kriging" in the kriging/geostatistics literature (Cressie 1991, Meiring et al 1998).

On the subject of spatial estimation, the U.S. National Acid Precipitation Assessment Program (NAPAP) evaluation found that the EMEFS field monitoring data were quite "noisy" across space and time. Rather than impose an empirically driven model to smooth the spatially noisy EMEFS data, the model evaluation team elected to reduce the noise, to provide for more stringent testing, by forming regional groups of sites and averaging the EMEFS data over the sites in each region (Dennis et al 1993). This *is*, in fact, an empirically driven (model) smoothing of the EMEFS data, but at a very course spatial scale defined by 9 regions of varying spatial extent covering most of the eastern half of the US. We believe that a much more stringent test is provided by "appropriate" smoothing of the data at the grid-cell level in the sense of statistically "optimal" estimation of grid-cell averages.

Recent examples of the application of EPA-recommended procedures in the U.S. include evaluations of a number of models for the Lake Michigan Ozone Study (Hanna et al. 1996) and the evaluation of the UAM-V model for the Northeast region of the U.S. by the Ozone Transport Assessment Group (OTAG). See http://capita.wustl.edu/OTAG/Reports/Sonoma/Report2.1.html and http://www.epa.gov/ttn/otag/finalrpt/.

Procedures similar to these have been used in Europe for evaluation of a variety of regional air quality models. In Hass et al (1995), evaluating the EURAD model, observations at monitoring sites are compared with model predictions derived from bilinear interpolation of neighboring grid cells. In Hass et al (1997), which considers the EMEP, EURAD, LOTOS, and REM3 models, observations are compared with model predictions for the nearest grid cell.

3. New operational evaluation proposals

3.1 First order assessment: statistical modeling and estimation of grid cell average concentrations

The calculation of estimates of average ozone concentrations over grid cells for comparison with photochemical model predictions requires a spatio-temporal statistical model. In principal, a number of spatio-temporal modeling methods proposed in the recent statistical literature might be applied, although the complexities of the characteristics of hourly ozone monitoring data limit some of these options. Meiring et al (1998) briefly reviews the models of Carroll et al (1997), Wikle (1996), and Wikle and Cressie (1997), which are most relevant for comparison with our approach. Our analyses are based on the representation of ozone observations in terms of a long-term mean trend in the diurnal hourly variation in ozone concentrations and the statistical characterization of the spatio-temporal correlation of the deviations from the long-term trend. Other recent spatio-temporal analyses based on this general approach include those of Høst et al (1995) and Brown, Le and Zidek (1994). For ozone, the spatio-temporal deviations from long-term mean trends have quite complex structure as their temporal and spatial aspects are not at all separable. We find that: (1) the short-lag temporal correlations display a periodically varying structure on a diurnal basis; (2) the temporal correlation structure of the monitoring site specific time series of residuals varies in space; and (3) the local spatial correlation structure of the corresponding series of residuals at neighboring sites varies in space—that is, the spatial correlation structure is non-stationary (Meiring et al 1998). This third feature is of particular interest and is discussed further in the next section on spatio-temporal correlation structure.

Guttorp et al. (1994) and Meiring et al. (1998) demonstrate an analysis using a spatio-temporal model to estimate grid cell averages for comparison with SARMAP model predictions for the San Joaquin Valley. The first panel of Figure 1, taken from Meiring et al. (1998), shows a 2-month time series of model predictions for a particular grid cell and corresponding hourly grid cell estimates with standard error bars (which do not happen to account for the uncertainty in the mean field). Observations at 3 monitoring sites in or near the target grid cell are plotted along with the SARMAP model predictions for that grid cell in the second panel. Conventional practice has usually been to compare the individual monitoring site observations with the model prediction curve as in the second panel of Figure 1, without the benefit of any uncertainty bars—statistical standard errors for the observations, or sensitivity bars for the model predictions. Because of the difference is spatial support—point vs. grid cell—statistical summaries derived from these comparisons are difficult to interpret.

3.2 Second order assessment: comparison of spatio-temporal correlation structure

Commonly computed numerical summaries of comparisons between grid cell model predictions and point monitoring data can be insufficient for model assessment, and possibly even misleading, particularly when model parameters and inputs have been adjusted so that predictions better match monitoring data. We suggest that more diagnostic information is available through consideration of the multivariate nature of the modeled and observed spatial fields and through consideration of the second order properties of these fields (cf. Dennis et al 1990).

As explained in our recent publications on the estimation of nonstationary spatial covariance structure, we expect patterns of spatial covariance to vary from point to point for most spatial-temporal environmental processes because of the spatially varying effects of orography and meteorology. The spatial covariance structure provides a global perspective of the dynamic behavior of the underlying process as expressed in the second order stochastic properties of the spatio-temporal pollution field. We depict the nature of this spatial covariance structure graphically using biorthogonal grids (Sampson and Guttorp 1992, Sampson et al 1991).

Figure 2 presents the result of an analysis of the spatial correlation structure for daily 2 p.m. ozone measurements in the San Joaquin Valley over a two-month period in the summer of 1990. The statistical model for spatial correlation structure is based on a spatial deformation of the geographic coordinate system in which pairs of monitoring sites that are relatively highly correlated appear relatively closely located while weakly correlated pairs are further apart, in comparison with their geographic positions. The statistical model is assumed stationary or homogeneous in terms of this deformed coordinate system. For these new coordinates (not shown in Figure 2), variances of differences in observations between sites, which we call *spatial dispersions*, are plotted against intersite distances as shown in the first panel of Figure 2 with a fitted exponential variogram. The second panel of Figure 2 presents a *biorthogonal grid*, a sampling of the local principal axes (affine derivative) of a nonlinear mapping between the geographic and new coordinate systems. The curves running generally northwest–southeast indicate the local directions of strongest spatial correlation while the orthogonal curves represent the local directions of weakest correlation. The empirically computed directions of strong correlation align roughly with the San Joaquin Valley and the directions of the principal wind patterns, as one would expect.

Because biorthogonal grids reflect the underlying meteorology and environmental processes, it should be useful to know how well the structure manifest in the observational data is also represented by the model predictions. Of course, in order to be able to carry out such an analysis it is necessary to have both sufficient temporal model output for estimation of this correlation structure and numerical procedures for doing so. Photochemical models producing predictions at smaller spatial scales (4-12 km in the case of the SARMAP Air Quality Model) are typically run only to simulate certain multi-day high ozone episodes. These do not provide time series of sufficient length to estimate correlation structures corresponding to those that can be estimated from much longer monitoring observation series. In addition, the number of spatial locations (grid cells) at which model predictions are produced is generally much greater than the number of point monitoring sites, and the fitting of our nonstationary spatial covariance models to such a large spatial network poses additional challenges which we are just beginning to address. Nonetheless, we ask the reader to imagine a similar calculation and analysis derived from model output and the comparison of two such correlation structures, one representing the field monitoring data and one representing the model output, as drawn in Figure 2.

3.3 Diagnostic display of spatial patterns in prediction errors

The EPA-recommended statistical measures presented above do not appear to be particularly helpful diagnostically. They provide a variety of measures of difference between observations and model predictions, but they provide little indication of how well spatio-temporal patterns of ozone concentrations are represented or what the spatial structure of the prediction errors is. We suggest here two possible diagnostic displays.

Differences between maps of model predictions and maps computed from data-based grid cell estimates (section 3.1) yield a spatial difference field. As many authors have noted, it is important to study the spatial pattern of these differences. To date, investigation of spatial patterns have been primarily by visual inspection and comparisons of the locations of peak concentrations. We suggest a more comprehensive analysis with two different decompositions of the difference field between observations and predictions.

One approach is based on the decomposition of spatial response surfaces in terms of "principal warps" as introduced by Bookstein (1989). The total difference field, evaluated either at the monitoring sites or on all the grid cells of the modeling domain, is decomposed into a global linear trend (if any) and a sequence of nonlinear patterns of successively smaller spatial scales. There will likely be large scale nonlinear differences in the spatial maps computed from the observational data and the model predictions as well as localized errors. In particular, the error in location of the region of peak ozone concentration may be consistent with a global error pattern or it may be a localized (perhaps less important) error. This analysis will yield both a graphical and numerical decomposition of these components of error. These decompositions of error may be integrated over time for total summary measures.

Calculation of this decomposition involves a straightforward eigenanalysis of the "bending energy matrix" underlying the representation of the error field as a smooth surface using a thin-plate spline interpolation (Bookstein 1989, Sampson et al 1991). The components of varying spatial scales are also described as components of the spline of varying bending energy, with higher bending energy being associated with small spatial scale features of curvature in the error field. We believe that this decomposition may provide an analysis of the error field that is more relevant to the purposes of model evaluation than what might be considered as competing approaches: decompositions in terms of spatial polynomial components, Fourier components, or empirical orthogonal function (EOF) analysis in the spatial literature. (See the appendix to Ludwig (1994) for one presentation.)

A second approach to a diagnostic analysis of spatial patterns in errors considers the following question: can iso-concentration contours determined by spatio-temporal analysis and interpolation of field monitoring observations be represented, in part, as a spatial perturbation of (or error in) corresponding contours determined from the model predictions? That is, can we point not only to the error in the location of, say, the maximum ozone concentration, but can we more generally identify spatial errors in the locations of the iso-concentration contours or the spatial gradients in concentration fields? Methods for computing deformations of one image to approximately match another, commonly computed now in certain fields of medical imaging (see, e.g., Gee and Haynor, to appear) can be applied here to compute a *spatial deformation field* that decomposes the difference between predicted and observed concentration fields into one component that is purely spatial and a residual representing errors in levels after spatial registration.

Figure 3 presents an illustration of this type of decomposition. Panel (a) shows a shaded contour plot computed from a simple spatial interpolation of observations taken at 4 p.m. on day 3 of the targeted high ozone episode of the summer of 1990. In all four panels of Figure 3, contours have been drawn at ozone concentrations of 40, 80, and 120 ppb, the latter being the 1 hour maximum ozone limit in the U.S. National Ambient Air Quality Standards. Panel (b) shows a corresponding contour map for the SARMAP model predictions. The simple sum over the grid cells of the squared differences between these two fields is approximately 554900 ppb^2. A smooth spatial deformation of the map of predicted concentrations was then computed to better align the predictions with the map computed from the observations. The nature of the deformation is indicated by the arrows drawn on panel (b). We then show panel (a) again drawn next to the spatially displaced model predictions in panel (c); the sum of squared differences between these two maps is now only 55650 ppb^2, a decrease by nearly a factor of 10. Thus the total squared error *can be* decomposed into a dominant component of "spatial error" and a smaller residual component. Figure 3 is presented here only for purposes of demonstration; we will not discuss the details of the calculations of the deformation. This decomposition is not unique, and it does not guarantee a scientifically valid explanation. Nonetheless, we suggest that the deformation field indicated by the arrows on panel (b) be studied for possible interpretation of model errors as being due to factors such as transport errors. These calculations can be extended to 3D deformations of the observed and predicted spatio-temporal fields, although illustrating and interpreting the results would pose a new challenge.

4. Discussion

The first of the procedures recommended above, spatial estimation of grid cell averages, was intended to put model–observation comparisons on a sound statistical basis with interpretable standard errors of estimation. We hope that our second and third proposals will lend further diagnostic insight into the spatio-temporal comparison of model predictions and field observations. Further algorithmic development is necessary to make routine implementation of these ideas feasible.

Acknowledgement

Early development of these ideas was sponsored in part by a research contract with the Electric Power Research Institute, Palo Alto, California. The current research is supported by a cooperative agreement between the US Environmental Protection Agency and the National Research Center for Statistics and the Environment at the University of Washington. It has not been subjected to agency review and does not necessarily represent the policies or practices of the U.S. Environmental Protection Agency.

References

Brown PJ, Le N, Zidek JV 1994 Multivariate spatial interpolation and exposure to air pollutants. Canad J Statist 22:489-509.

Carroll RJ, Chen R, Li TH, Newton HJ, Schmiediche H, Wang N, George EI 1997 Trends in ozone exposure in Harris County, Texas. J Amer Statist Assoc 92:392-415 (with discussion).

Code of Federal Regulations (Title 40, part 50): Protection of the Environment; National Primary and Secondary Ambient Air Quality Standards.

Code of Federal Regulations (Title 40, part 51): Protection of the Environment; Requirements for Preparation, Adoption, and Submittal of Implementation Plans. Appendix W: Guideline on Air Quality Models.

Cressie NAC 1991 Statistics for Spatial Data. John Wiley and Sons, New York.

Dennis RL, Barchet WR, Clark TL, Seilkop SK 1990 Evaluation of regional acidic deposition models (Part 1), NAPAP SOS/T report 5. In: National Acid Precipitation Assessment Program: State of Science and Technology, Vol 1, National Acid Precipitation Assessment Program, Washington, DC.

Dennis RL, McHenry JN, Barchet WR, Binkowski FS, Byun DW 1993 Correcting RADM's sulfate underprediction: discovery and correction of model errors and testing the corrections through comparisons against field data. Atmos Environ 27A:975-997.

Environmental Protection Agency 1994 Guidance on Urban Airshed Model (UAM) Reporting Requirments for Attainment Demonstration, EPA-454/R-93-056.

Gee JC, Haynor D Numerical methods for high-dimensional warps. In: Toga AW (ed) Brain Warping, Academic Press, San Diego, to appear.

Guttorp P, Sampson PD 1994 Methods for estimating heterogeneous spatial covariance functions with environmental applications. In: Patil GP, Rao CR (eds) Handbook of Statistics XII: Environmental Statistics, Elsevier/North Holland, New York p 663-690.

Guttorp P, Meiring W, Sampson PD 1994 A space-time analysis of ground-level ozone data. Environmetrics 5:241-254

Hass H, Jakobs HJ, Memmesheimer M 1995 Analysis of a regional model (EURAD) near surface gas concentration predictions using observations from networks. Meteorol Atmos Phys 57:173-200.

Hass H, Builtjes, PJH, Simpson D, Stern R 1997 Comparison of model results obtained with several European   regional air quality models. Atmos Environ 31:3259-3279.

Hanna SR, Moore GE, Fernau ME 1996 Evaluation of photochemical grid models (UAM-IV, UAM-V, and the ROM/UAM-IV couple) using data from the Lake Michigan Ozone Study (LMOS). Atmos Environ 30:3265-3279.

Host G, Omre H, Switzer P 1995 Spatial interpolation errors for monitoring data. J Amer Statist Assoc 90:853-861.

Hwang D, Byun DW, Odman MT 1997 An automatic differentiation technique for sensitivity analysis of numerical advection schemes in air quality models. Atmos Environ 31:879-888.

Lefohn A, Roth P, Ziman S 1998 The proposed standard for ozone: The feasibility of attainment and the role of modeling in planning. NARSTO White Paper (http://odysseus.owt.com/Narsto/scienceforum.html).

Ludwig FL 1994 A procedure for determining representative monitoring sites for photochemical model evaluation studies. In: Solomon PA, Silver TA (eds) Planning and Managing Air Quality Modeling and Measurement Studies: a Perspective through SJVAQS/AUSPEX. Lewis Publishers/Pacific Gas and Electric Company, Chelsea, MI, USA, p 597-615.

McNair LA, Harley, RA, Russell AG 1996 Spatial inhomogeneity in pllutant concentrations, and their implications for air quality model evaluation. Atmos Environ 30:4291-4301.

Meiring W, Guttorp P, Sampson PD 1998 Space-time estimation of grid-cell hourly ozone levels for assessment of a deterministic model. Environ Ecol Statist, in press.

Meng Z, Dabdub D, Seinfeld JH 1998 Size-resolved and chemically resolved model of atmospheric aerosol dynamics. J Geophys Res 103 (D3):3419-3435.

National Research Council 1991 Rethinking the Ozone Problem in Urban and Regional Air Pollution. National Academy Press, Washington DC

Sampson PD, Guttorp P 1992 Nonparametric estimation of nonstationary spatial covariance structure. J Amer Statist Assoc 87:108-119

Schere KL 1988 Ozone air quality models: critical review discussion papers. J Air Poll Ctrl Waste Mgmt 38(9):1114-.

Seinfeld JH 1988 Ozone air quality models: A critical review. J Air Poll Ctrl Waste Mgmt 38(5):616-647.

Solomon PA, Silver TA (eds) 1994 Planning and Managing Air Quality Modeling and Measurement Studies: a Perspective through SJVAQS/AUSPEX. Lewis Publishers/Pacific Gas and Electric Company, Chelsea, MI, USA

Solomon PA, Thuillier A 1995 SJVAQS/AUSPEX/SARMAP 1990 Field Measurement Project v 2. Field Measurement Characteristics. PG&E report 009.2-94.1, Dept. of Research and Development, San Ramone, CA

Wikle CK 1996 Spatio-temporal statistical models with applications to atmospheric processes, PhD dissertation, Dept of Geological and Atmospheric Sciences, Iowa State Univ, Ames, IA.

Wikle CK, Cressie NAC 1997 A dimension-reduction approach to space-time Kalman filtering. Preprint No. 97-24, Statistical Laboratory, Iowa State University, Ames, IA.

Figure Legends

Figure 1. Comparison of model output and an estimate of ozone concentration for one grid cell for the 4 days where model output was available. The solid line in the top figure represents the estimated ozone level for one grid cell in the Sacramento region of California. The dotted lines above and below the solid line show the areal estimate ± two standard errors. The broken line shows the model output. The lower plot shows time series of the observed ozone at three monitoring sites in and near this grid cell. The horizontal line in each of the panels indicates the ozone air quality limit of 120 ppb. (Figure taken, with permission, from Meiring et al. 1998.)

Figure 2. The curves drawn in this figure are *biorthogonal grids* for a thin-plate spline mapping the geographic coordinates of 100 San Joaquin Valley monitoring sites into the deformed coordinate system representing the nonstationary spatial correlation

structure of the ozone observations taken at 2 p.m. each day over 2 months. These are a sampling of the affine derivative of the nonlinear mapping. The curves are coded according to the value of the derivative which represents the local shrinking or stretching relative to the geographic map. Curves running generally northwest–southeast are directions of greatest relative shrinkage and correspond to directions of highest spatial correlation. These are aligned generally with the San Joaquin Valley and the directions of the predominant winds. The orthogonal curves represent the directions of weakest spatial correlation.

Figure 3. Shaded contour plots of observed ozone concentrations and model predictions with contours drawn at 40, 80, and 120 ppb. (a) Interpolated ozone concentrations for 4 p.m. observations on day 218 of 1990; (b) SARMAP air quality model predictions for the same hour and day with a sampling of vectors indicating the smooth deformation field computed to approximately align the concentrations in panel (b) with those in panel (a); (c) Spatial deformation of the predicted concentration field which agrees well with the observed concentrations of panel (a).

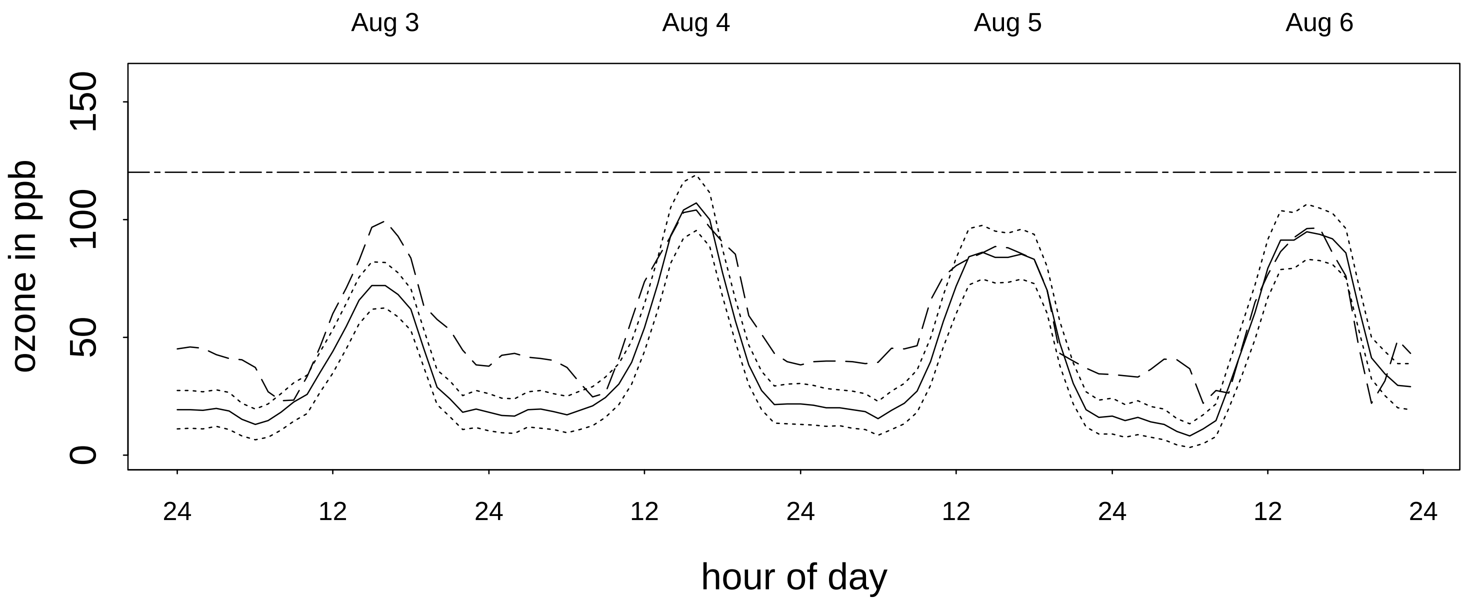
Aug 3
Aug 4
Aug 5
Aug 6
ozone in ppb
0
50
100
150
24
12
24
12
24
12
24
12
24
hour of day

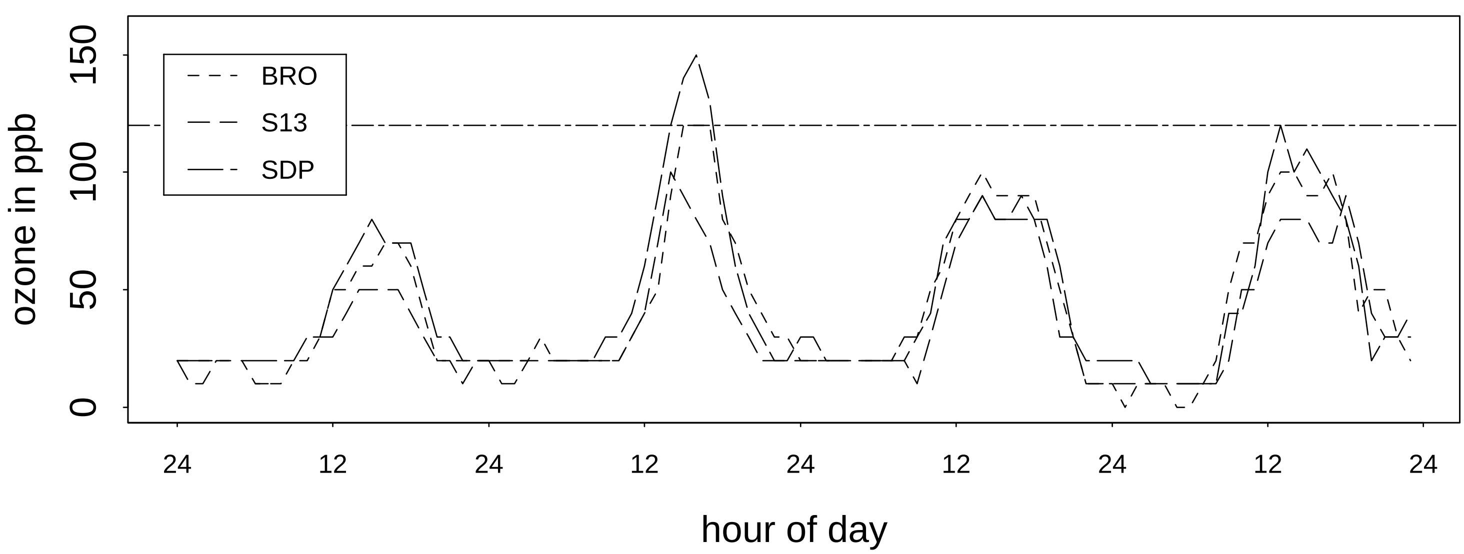
BRO
S13
SDP
ozone in ppb
0
50
100
150
24
12
24
12
24
12
24
12
24
hour of day

Hour 14

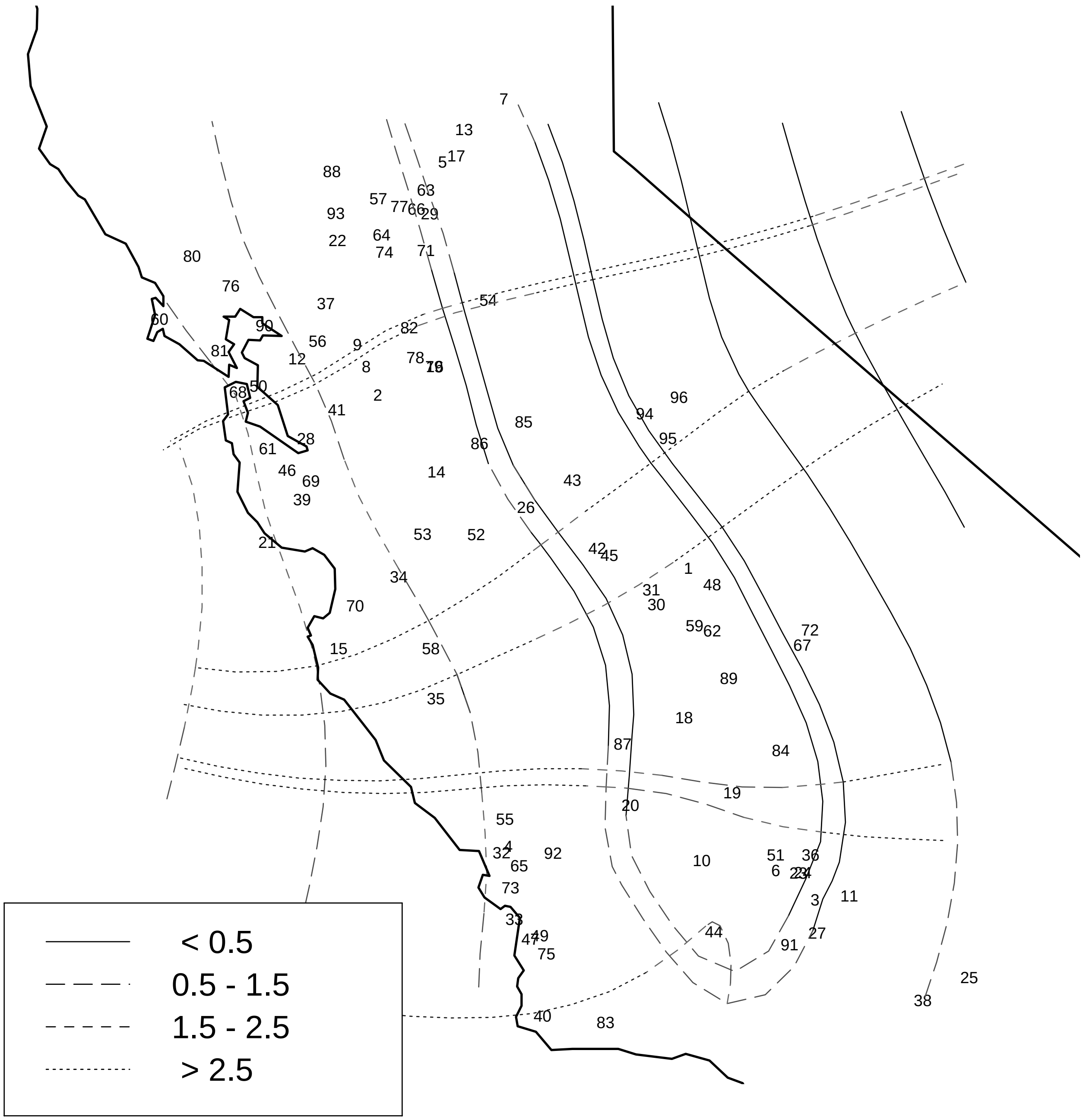

7
13
5
17
88
63
57
77
66
29
93
64
22
74
71
80
76
37
54
60
90
82
56
81
12
9
78
8
50
68
2
96
41
94
85
86
95
28
61
46
14
43
69
39
26
53
52
21
42
45
1
34
31
48
30
70
59
62
72
67
15
58
89
35
18
87
84
19
20
55
4
32
92
65
10
51
36
6
73
3
11
33
44
49
47
27
75
91
25
38
40
83
< 0.5
0.5 - 1.5
1.5 - 2.5
> 2.5

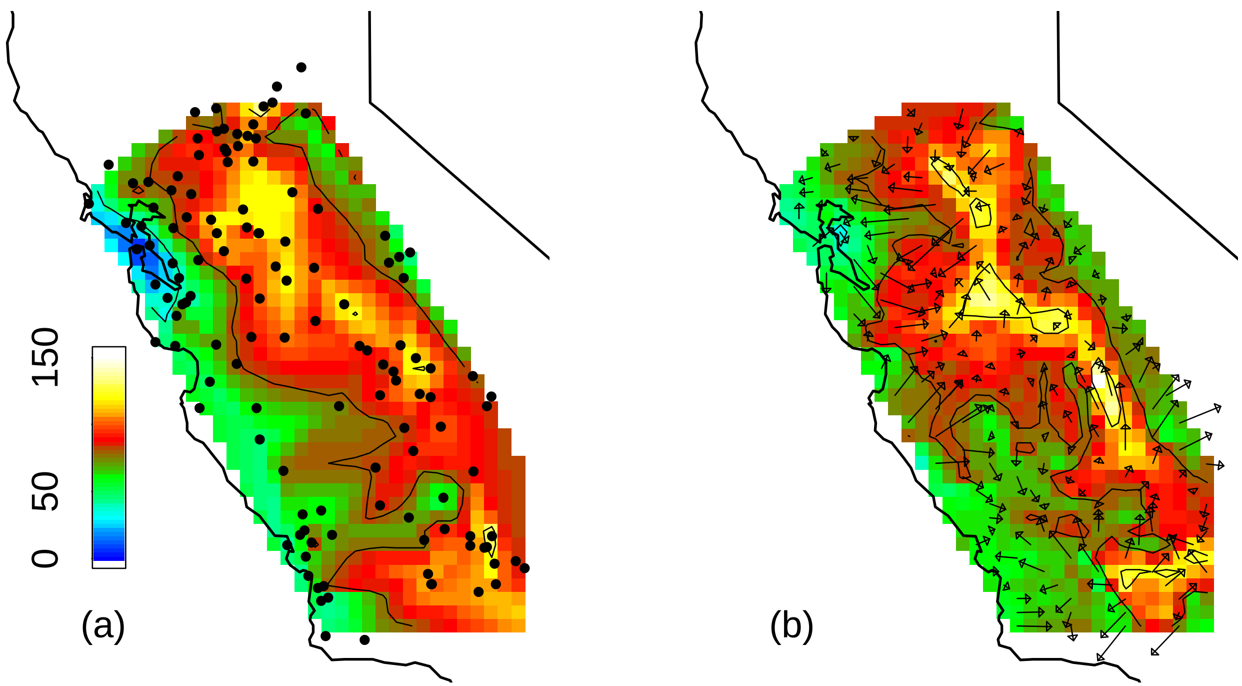

150
50
0
(a)
(b)

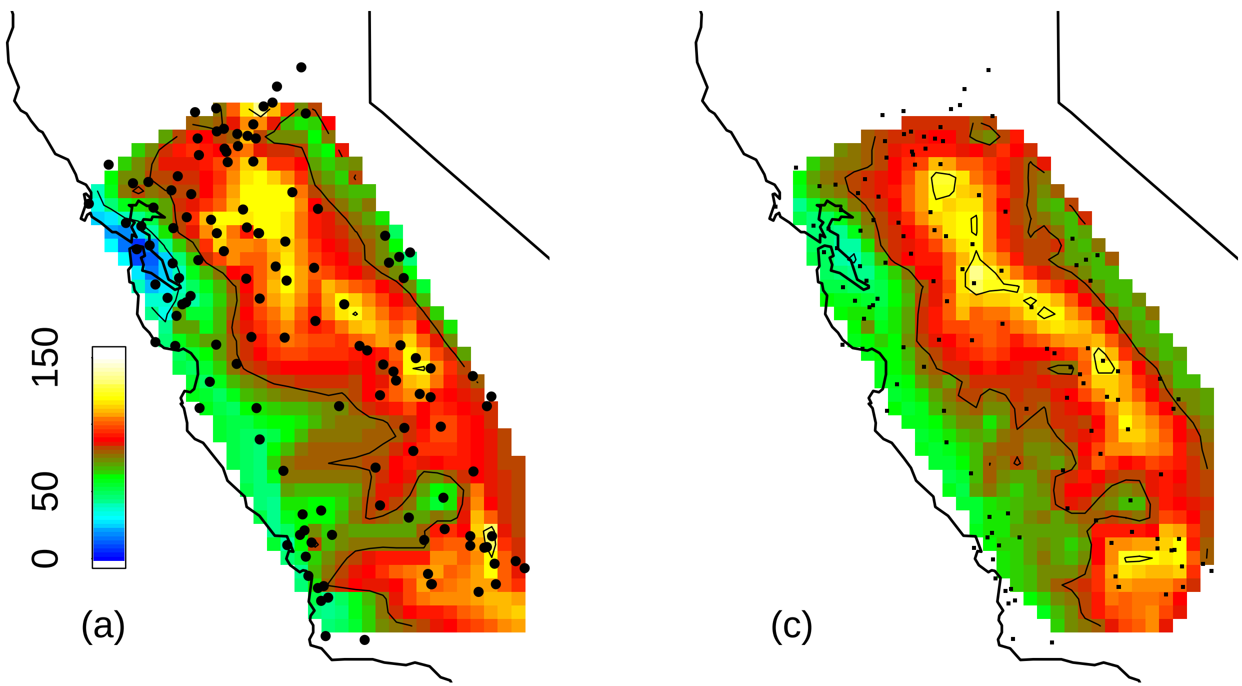
150
50
0
(a)
(c)